# Radial piezoelectric magnetic fans (RPMF) mathematical model development and design optimization for electronics cooling

Fadhilah Abdul Razak [a,*], Robiah Ahmad [a,*], Shamsul Sarip [a], Firdaus Muhammad-Sukki [b,c,*]

[a] *Razak Faculty of Technology and Informatics, Universiti Teknologi Malaysia, 54100 Jalan Sultan Yahya Petra, Kuala Lumpur, Malaysia*
[b] *School of Computing, Engineering & the Built Environment, Merchiston Campus, Edinburgh Napier University, 10 Colinton Road, Edinburgh EH10 5DT, UK*
[c] *Solar Research Institute (SRI), School of Electrical Engineering, College of Engineering, Universiti Teknologi MARA (UiTM), Shah Alam 40450, Malaysia*

ARTICLE INFO

ABSTRACT

Nowadays, almost everything was run by electronic-based devices regardless of its size and applications, functioning for kids to adults and operating throughout the days and nights. It is critical to manage the electronic thermal management to sustain the electronic device for longer period. This paper enhances the design of multiple piezoelectric magnetic fans (MPMF) to achieve maximum thermal efficiency. Some geometric parameters were investigated such as the magnet location, $x$, distance between magnets, $d$, and the orientation, $\theta$ of the fans. Response Surface Method (RSM) was used as optimization tool. Therefore, this paper presents a mathematical model of MPMF to predict the maximum fan deflection by optimizing the value of $x$, $d$, and $\theta$. The experimental results showed that the optimal value of $x$ was 44 mm from the origin, the range of $d$ value was in the range of 14.5 mm to 15.6 mm and in overall, fan deflection of radial piezoelectric magnetic fans (RPMF) was better than array piezoelectric magnetic fans (APMF). The most consistent average fan deflection was 11.6 mm at $d = 14.5$ mm and resonant frequency, $f_r = 42.66$ Hz. The Reynolds number, $Re$ for RPMF has increased from 437 to 577 (improved by 32 %) compared to APMF. The heat convection coefficient, $h$, for RPMF has improved 8.07 % from 32.96 to 35.62 and the thermal resistance reduced by 7.6 % from 1.58 to 1.46 which led to 5 % increment of overall thermal efficiency, 63 %. This clearly shows that the thermal efficiency has been improved by optimizing the $x$, $d$ and $\theta$ values of the MPMF.

## 1. Introduction

Nowadays, almost everything was run by electronic-based devices regardless of its size and applications, functioning for kids to adults and operating throughout the days and nights. The devices could be used nonstop by the users and if the heat dissipation system is not able to sustain the high temperature, this will harm the devices and cause failure due to overheating [1]. The allowable temperature for electronic components is in range of 50–60 °C [2], and 60–100 °C for computer chips [3]. If devices operate beyond the allowable temperature, the devices might overheat. As the medium, air was preferred due to its high reliability and environmentally favorable [4]. Implementation of

intelligent material piezoelectric in electronics thermal management has attracted many ideas on how to overcome the drawbacks from existing cooling fan into an intelligent cooler that is able to meet the requirement in both cooling and power reduction. The piezoelectric material acts as an actuator to convert electrical energy into mechanical energy in terms of vibration. The vibration is considered huge which able to disturb the surrounding air-flow. The level of disturbance will determine the efficiency of piezoelectric actuator in cooling system. The piezoelectric actuator can be integrated with other cooling method such as piezoelectric droplet generator [5], synthetic jet [6], dual plate piezoelectric cooling jet [7], micro-blower [8] and piezoelectric fan [9].

The piezoelectric fan has several advantages compared to

conventional fans such as low power consumption [10], low noise [11] and light in weight [12]. It is found that the heat removal by piezoelectric fan depends on the velocity and dispersion of air streams [13] and the air velocity is influenced by the running frequency and the fan deflection [14]. Other influencing factors including the orientation of the piezoelectric fan with respect to the heat source [15], the material of the flexible blade [16,17,18], fan dimension [19] and fan tip gap to the heat source [20,21].

The performance of the piezoelectric fan could be enhanced with additional piezoelectric fan to gain greater fan deflection either using same piezoelectric fans [22] or passive fans [23]. A multiple piezoelectric magnetic fans (MPMF) was introduced by Ma et al. [24]. The fan blades oscillated due to magnets that attached on each fan. The magnets were glued on the flexible blades in such a way that the repulsive magnetic force was generated from the piezoelectric fan and transferred the energy to the adjacent fans [25–27] so that all the blades deflected together. Similar to what has been done with the single piezoelectric fan, further research should be conducted to understand the structural and dynamic features of MPMF and the flow fields generated around them. The distance between magnets needs to be precisely measured as it determines the amount of fan deflection that further affect the performance of heat removal [28]. The mechanism of MPMF deals mainly with magnetic force, then all the parameters that relate to the magnetic force would be significant and become contributing parameters to the MPMF. The MPMF should be located near to the heat source and close to the exit so that the air is not circulating around the heating area that affect the thermal efficiency [29].

The strength of the piezoelectric actuator is the key performance of the whole system besides the repulsive magnetic force from the magnets. Less driving force leads to poor air distraction thus, it is important to ensure an optimized dimension of piezoelectric fan and magnet [14,24,30] are selected with optimized location so that it deflects at widest amplitude with significant frequency.

Another factor to be considered is the orientation of the blades in the MPMF which influence the performance of MPMF. However, there is no comprehensive equation of deflection shows the relationship among the magnet location, $x$, distance between magnets, $d$, and the orientation, $\theta$ of the fans. There is also no comparison between array piezoelectric magnetic fans (APMF) and radial piezoelectric magnetic fans (RPMF) that gives better performance of cooling. The RPMF [31] showed increasing performance compared to single fan yet no comparison with other MPMF. Besides number of fans and width of the blades [31], the performance of the MPMF could also be improved based on the location of magnets [32], the distance between magnets and the orientation of the MPMF; by using Response Surface Method (RSM) in Design Expert (DE) in finding the optimal response for RPMF design so that the device functions at its maximum performance. DE is a statistical software package that combine a few methods of Design of Experiment (DOE) to propose the primary effect of each factor and their interaction besides having perfect tool for design, screening and optimization of experiment. DE proposes the number of test runs needed to determine the ideal values for each of the factors in the experiment. By adjusting the values of all elements simultaneously as well as the value of responses, the software calculates the major effects of each factor along with the interactions between factors. The optimal operating parameters for a process can be determined using the optimization feature.

The fundamental of RSM [33] has suggested a second-degree polynomial model for solving the multi-objective optimization problems. The approach gives results in approximated values, yet effective because the model is easy to estimate and apply. RSM also quantifies relationships among one or more output responses and the significant input factors. The justification of using the RSM in this study is that the MPMF require multiple responses from the experiments to find the optimal design of MPMF so that the cooling efficiency driven by MPMF can be reached proficiently. In RSM, Central Composite Design (CCD) is a common augment from the two-level factorial design selected to run the experiments.

Therefore, this paper is proposing an enhancement of parameters in RPMF using RSM to satisfy the high heat flux in the confined spaces of electronic devices in thermal management.

## 2. Design and fabrication of MPMF

A diagram of MPMF both in array and radial is shown in Fig. 1. The MPMF consisted of 5 parts: a round shape magnet, a piezoelectric actuator attached with mylar blade (fan No. 1), passive fans (fan No. 2,3,4 and 5) consisted of carbon fiber and mylar blade, mounting for each fan and the casing made from acrylic with thickness 3 mm. A dummy heat source was placed at the tip of the fans for thermal analysis. The heat source was made of ceramic plate and attached to aluminum heat sink (30 × 100 × 10) mm for better heat distribution (Fig. 2)

The piezoelectric actuator was bought from piezo systems website[1] with identification number of RFN1-005. The piezo fan consumes very small power; 30 mW and very light in weight for about 2.8 g. The fan is running with 115 VAC which is not equivalent with standard voltage used in this country (240 VAC). Thus, a custom-made step-down transformer was constructed. A function generator was utilized to activate the piezoelectric fan while adjusting the frequency of the fan. The frequency of the fan is commonly regulated to get its resonant frequency.

The fans need to have a mounting to hold the fan for safety and to avoid energy loss through vibration. The mounting was designed in such a way that it is stable and consumed less space. The fan was screwed to the mounting and the mounting was screwed to the casing. Screws are preferred to prevent misalignment which can affect the deflection of the fans. The mounting was screwed to the casing in a slot so that the mounting is easily can be dragged back and forth or to a certain distance between the fans. As for RPMF orientation, the fans were allocated in radial orientation, $\theta$ with angle of 60° as to investigate which orientation is optimum for MPMF.

The MPMF also equipped with casing which has inlet and outlet for air flow to get better result for thermal analysis. The casing was designed with dimension of (100 × 120 × 30) mm.

## 3. Experimental setup and procedure

In this research, two measurements were performed to synthetically investigate the performance of the MPMF, the driving performance of MPMF without a thermal load (including the average deflection of the MPMF with variation of location of magnet, distance between magnets both for APMF and RPMF, and the thermal management performance (including the temperature rising and thermal resistance measurements). The schematic diagram is shown in Fig. 3. The dimension of the fan was same like the driving fan. The power drive parts include an arbitrary waveform generator (INSTEK Model GFG-8020H) and a step-down transformer to change the running voltage of the piezoelectric fan from 115 VAC to 240 VAC. As the performance of MPMF depends on the average deflection of blades, which is affected by several parameters, the maximum average fan deflection was obtained by conducting RSM to run the experiments. By using RSM, the number of experiments was reduced yet still gain high reliability in the results. The experiments to determine the performance of MPMF without a thermal load were conducted based on factors and responses that have been decided earlier and constructed in matrix table (see Table 1). For Case 1, the factors (input) are the frequency offset and magnet location; the responses are fan deflection and air velocity whereas for Case 2, the factors are the frequency offset, fan orientation and distance between magnets. The responses are same with Case 1.

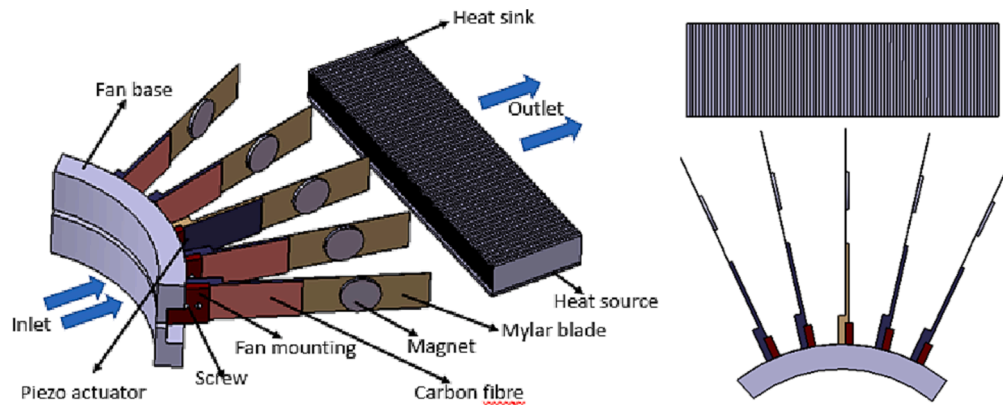The matrix table in the DE was developed by generalizing the magnet
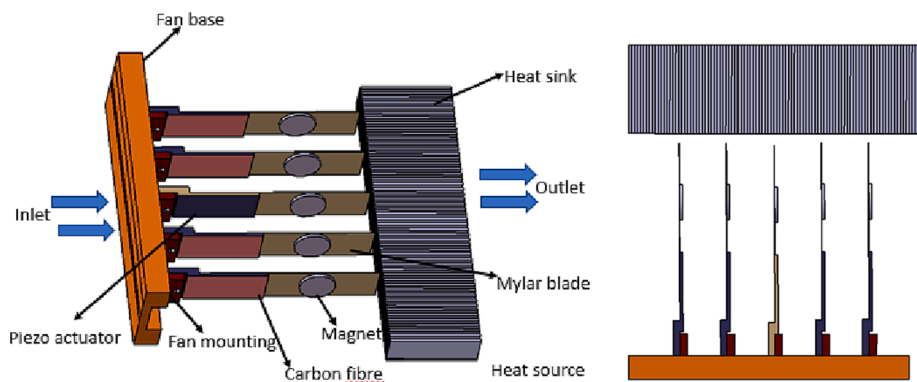
**Fig. 1.** Schematic diagram of RPMF.



**Fig. 2.** Schematic diagram of APMF.
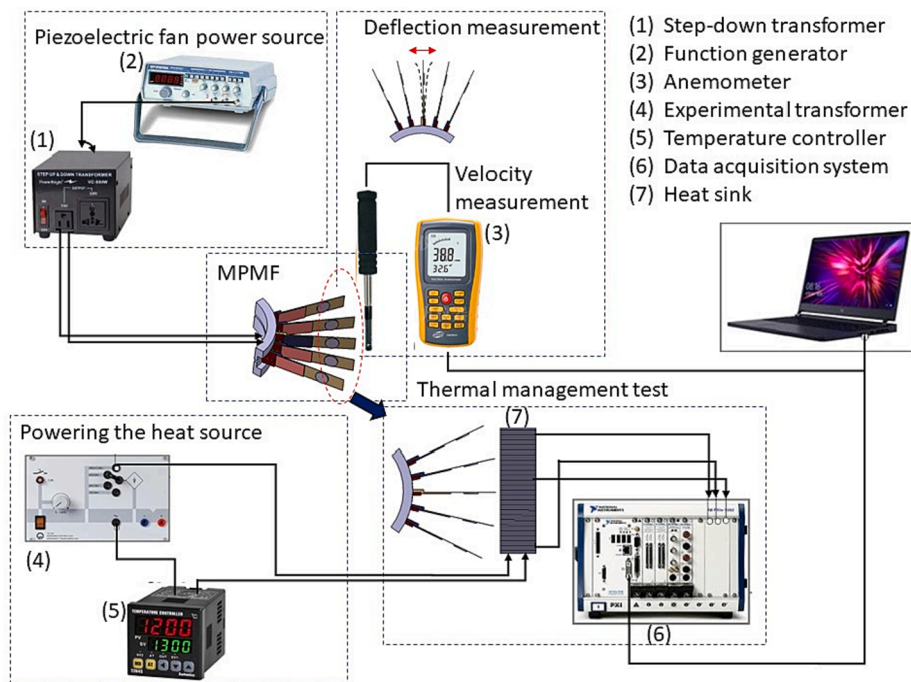


**Fig. 3.** Schematic diagram for deflection, velocity measurement and thermal management test of MPMF.

location as the ratio to the total length of the fan (69 mm) (later known as pitch) so that the mechanism could be applied for different size of fan. The measurement of the pitch was started from the mounting of the fan (refer Fig. 1). There are three pitches have been investigated which were 38 mm (55.1 %), 44 mm (63.8 %) and 50 mm (72.5 %). The distance between the magnets was measured from the centre of magnets. All the

**Table 1**

Factors and responses of the experiments.

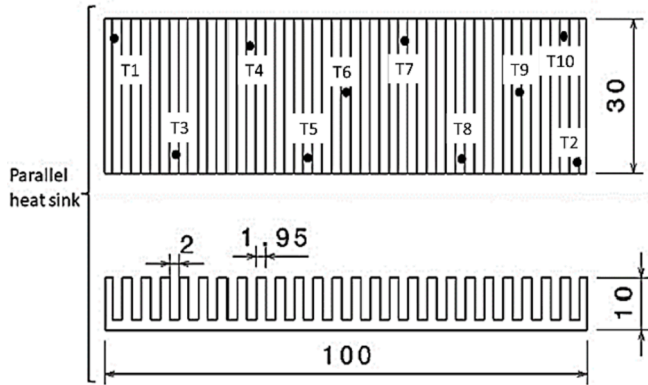| Level of value | High level | Low level |
|---|---|---|
| Frequency offset (%) | −5 | +5 |
| Location of magnet (%) | 55.1 | 72.5 |
| Distance between magnets (mm) | 14.9 | 26.9 |

*The values were taken from previous work carried out by the authors published in [9] which demonstrate significant fan deflection.



**Fig. 4.** Dummy heat source with thermocouples.

initial values were referred to [34] as this study is the continuation of the research paper.

A diagram of thermal management performance test part is combined in Fig. 3. The dummy heat source was controlled by an automatic temperature regulation system at certain maximum temperature so that the cooling operation would dominantly done by the MPMF. The dummy heat source is made up from ceramic (thermal conductivity of ≤ 5.077 W/mK) with 45 W power consumption and is attached to an aluminium heat sink (10 × 30 × 100) mm in dimension. The cooling was further enhanced by the MPMF. The MPMF has a closed casing that only has inlet and outlet for air flow.

The experiment was continued by varying the input power of the heat source and its equilibrium temperature was also recorded. The MPMF always running at its optimal design parameters. As for the temperature controller, it started to activate the heat source if the temperature of the heat source is below the equilibrium temperature. As the heat source was in steady state condition, MPMF cooling system was activated while the heat source was kept powered on. The condition remained until it reached equilibrium state again.

In the data acquisition part, ten thermocouples were employed to observe the performance of MPMF. Ten type-K thermocouples were put on the heat sink to monitor temperatures in the experiments. Of these, seven were mounted and the average reading on the exposed surface of the heat sink (Fig. 4) to calculate the average surface temperature. Two thermocouples were suspended in air near to the heat sink. Remaining thermocouple was used to monitor the ambient air temperature. The thermocouples were connected to NI DAQ for data collection. The thermocouples were located randomly in such a way that the performance of each of the fan can be diagnosed based on the temperature recording.

### 3.1. Data reduction

#### 3.1.1. Theoretical fan deflection

The deflection of fans in MPMF imitates the mechanism of pendulum and a beam with certain modifications. The deflection has produced a flow of air dispersion with certain velocity which improves the heat removal from hot spot area. At resonant frequency, the fan deflection will be at maximum [35] and less noise is generated [36]. Therefore, it is

**Table 2**

Some Constant Values Related to The Development of Mathematical Model.

| Item | Magnitude |
|---|---|
| $E_{piezo}e$ | $6.70 \times 10^{10} N/m^2$ |
| $E_{mylar}$ | $2.7 \times 10^9 N/m^2$ |
| $I_{piezo}$ | $1.70699 \times 10^{-10} m^4$ |
| $I_{mylar}$ | $4.33574 \times 10^{-11} m^4$ |
| $d_{31}$ | $1.90 \times 10^{-10}$ |
| $B_0$ (magnet N38) | $1.26$ Tesla |
| $\mu_0$ | $1.26 \times 10^{-6} N/A^2$ |

required to derive the MPMF related equation as a function of frequency for better control during the experiment. There are some constant values related to the development of mathematical model as stated in Table 2.

The equation of deflection for a piezoelectric actuator was taken from [37] which also has been implemented in MATLAB coding to calculate the deflection of piezoelectric actuator as shown in Equation (1).

$$\delta = \frac{-3d_{31}VL^2}{8H^2} \quad (1)$$

where $d_{31}$ is piezoelectric strain coefficient, $V$ is voltage supplied, $L$ is length of the piezoelectric material and $H$ is the height of each individual uniform layer of the piezoelectric fan. Since bimorph piezoelectric fan is used throughout this study, the value of $H$ is half of the total height or thickness. In a single piezoelectric fan, the net force acting on the fan is coming from the strength of the piezo itself. The air velocity is influenced by the running frequency and the fan deflection (wavelength) as indicated by Equation (2). The total distance traveled from initial point and back to the same point is defined as wavelength (Equation (3)). Therefore, the velocity of air generated at the tip of the fan can be calculated as;

$$v_{nett} = (frequency)(wavelength) = f_r\lambda \quad (2)$$

$$\lambda = 4 \times Amplitude = 4A = 2\delta \quad (3)$$

where $A$ is amplitude and measured from maximum swing position to the vertical line (centre) whereas $\delta$ is the displacement from peak-to-peak of the fan tip. This definition was supported by [38,39]. The fan deflection with a magnet attached on it is derived from the principle of a beam exerted force at a point. The findings of optimum location of magnet for MPMF has been discussed in detail in [32]. As revision, the equation of deflection by considering the location of magnet can be defined using Equation (4).

$$\delta_{nett} = f(freq, x) = \frac{\left[ F_{piezo} + \left( \frac{0.3131\left( \frac{6EI}{x^2(3l-x)} \right)}{f_r^2} \right) g \right] x^2(3l-x)}{6EI} \quad (4)$$

The deflection becomes the function of total force applied to the fan ($F$), the total length of the fan ($l$), the Young Modulus of the blade made of ($E$) moment of inertia ($I$) and location of magnet ($x$).

The MPMF cooling system is activated by transferring the repulsive magnetic force between the magnets located on the fan blade. The magnetic force, $F_{mag}$, differs with different fan since it depends on the amount of force acting on each fan. Basically, a piezoelectric fan attached with a magnet is affected by the direct adjacent fan only as approved by [29].

$$\delta_{nett, \ array} = \frac{\left[ F_{piezo} + F_{mag} \right] x^2(3l-x)}{6EI} \quad (5)$$

The deflection of MPMF ($\delta$) was also influenced by the orientation of the MPMF and this study focused on the array and radial orientations. The radial orientation has advantage on its net force since this type of

orientation can generate a centrifugal force ($F_c$) which improves the deflection of the fans. The optimization of MPMF parameters involves multiple interactions between factors such as the location of magnet, $x$, , the distance between magnets, $d$ and the orientation of the MPMF, $\theta$ thus the Equation (4) and Equation (5) need to be revised so that the fan deflection become the function of $x$, $d$ and $\theta$.

$$\delta_{nett,\,radial} = \frac{\left[F_{piezo} + F_{mag} + F_\theta\right]x^2(3l-x)}{6EI} \tag{6}$$

Based on Equation (6), the fan deflection was influenced by the force exerted due to the radial orientation. Therefore, $F_\theta = F_c = \frac{mv^2}{r}$, where the centripetal force, $F_c$ has added up the exerting force to increase the deflection of the MPMF in radial orientation (RPMF). $v$ is the velocity of the fan and $r$ is the radius of the RPMF design. By comparing the Equations 5 and 6, it shows that RPMF has extra force to drive the MPMF in greater velocity thus help to remove the heat better compared to APMF.

The magnetic force, $F_{mag}$ for each fan (APMF and RPMF) was assumed to be disseminated evenly to the adjacent fans [29]. The piezoelectric fan (driving fan) was affected by magnetic force from its adjacent fans whereas the last fan was only affected by magnetic force of single fan. The interaction of magnets in MPMF was thoroughly explained in [40]. Equation (7) describes the magnetic force that applied on the piezoelectric fan.

$$F_{mag,1}(d) = \frac{1}{2}(F_{2-1}(d) + F_{3-1}(d)) = \left[\frac{B_0^2 A_{mag}^2 (t_{mag}^2 + r_{mag}^2)}{\pi \mu_0 t_{mag}^2}\right]\frac{1}{2}\left(\begin{array}{c}\left[\frac{-1}{d_{2-1}^2} - \frac{1}{(d_{2-1} + 2t_{mag})^2} + \frac{2}{(d_{2-1} + t_{mag})^2}\right] \\ + \left[\frac{-1}{d_{3-1}^2} - \frac{1}{(d_{3-1} + 2t_{mag})^3} + \frac{2}{(d_{3-1} + t_{mag})^3}\right]\end{array}\right) \tag{7}$$

On the other hand, Equation (8) shows the last fan was influenced by a single fan only.

$$\begin{aligned}F_{mag,5}(d) &= \frac{1}{2}(F_{5-3}(d)) \\ &= \left[\frac{B_0^2 A_{mag}^2 (t_{mag}^2 + r_{mag}^2)}{\pi \mu_0 t_{mag}^2}\right]\frac{1}{2}\left(\left[\frac{-1}{d_{2-1}^2} - \frac{1}{(d_{2-1} + 2t_{mag})^2}\right.\right. \\ &\quad \left.\left. + \frac{2}{(d_{2-1} + t_{mag})^2}\right]\right)\end{aligned} \tag{8}$$

The location of magnet is very important as it determines the maximum deflection of MPMF. A first mode resonant frequency is put into consideration since least noise is formed at this mode. The optimal location of magnet is the point that produced the highest velocity at the tip of the fan. The optimal location magnet also can determine the value of the stiffness of the fan (Equation (9)). The resonant frequency of single fan and multiple fans is different due to dissimilar acting net force on each system. Acting force for a single piezoelectric fan is due to the conversion energy from electrical energy to mechanical energy only. As for the MPMF, the acting force is also contributed by the magnetic force. The maximum deflection would occur at resonant frequency of the system. The resonant frequency of MPMF, $\omega_{piezo}$ is mainly influenced by mode shape, $\sigma$, total magnetic stiffness, $k_{eff}$ and total mass, $m_{eff}$ applied on the fan (Equation (10))

$$k_{piezo} = \frac{6EI}{x^2(3l-x)} = \frac{Etw^3}{2x^2(3l-x)} \tag{9}$$

$$\omega_{piezo} = 2\pi f_r = \frac{\sigma^2}{2\pi}\sqrt{\frac{k_{eff}}{m_{eff}}} = \frac{\sigma^2}{2\pi}\sqrt{\frac{k_{piezo} + k_{mag}}{m_{mag} + 0.24m_{piezo}}} \tag{10}$$

Additional parameter for MPMF is the magnetic stiffness whose fan is integrated from the force generated by the piezoelectric fan. Therefore, the magnetic stiffness for fan (1) is

$$K_{mag,1}(d) = \frac{1}{2}(k_{2-1}(d) + k_{3-1}(d)) \tag{11}$$

The resonant frequency of the piezoelectric fan was taken at its first mode shape ($\sigma = 1.875$) since none or less noise was produced at this mode shape. The deflection of vibrating plate was affected by the length of the vibrating plate, $l$, the location of magnet, $x$ and total force exerted to the plate (Mylar), $F_{nett}$. In this study, the length of the vibrating plate is made constant. As the magnet located nearer to the end of the beam, the deflection becomes greater, but the frequency of the piezoelectric fan become smaller. The significance of the magnet can be realized when MPMF were applied. For every single piezoelectric fan equipped with passive fan at the right and left side, total force exerted to the piezo-electric fan is accumulated from piezoelectric force, $F_{piezo}$ and magnetic force, $F_{mag}$ from the passive fans. Therefore, the final equation of deflection for fan (1) in array orientation (APMF) is shown in Equation (12) and radial orientation (RPMF) in Equation (13).

$$\delta_{f1,\,array} = \frac{\left[\frac{-9d_{31}VEI}{8H^2L} + \left[\frac{B_0^2 A_{mag}^2 (t_{mag}^2 + r_{mag}^2)}{\pi \mu_0 t_{mag}^2}\right]\frac{1}{2}\left(\begin{array}{c}\left[\frac{-1}{d_{2-1}^2} - \frac{1}{(d_{2-1}+2t_{mag})^2} + \frac{2}{(d_{2-1}+t_{mag})^2}\right] \\ + \left[\frac{-1}{d_{3-1}^2} - \frac{1}{(d_{3-1}+2t_{mag})^3} + \frac{2}{(d_{3-1}+t_{mag})^3}\right]\end{array}\right)\right]x^2(3l-x)}{6EI} \cdot \frac{1}{6EI} \tag{12}$$

$$\delta_{f1,\,radial} = \frac{\left[\frac{-9d_{31}VEI}{8H^2L} + \left[\frac{B_0^2 A_{mag}^2 (t_{mag}^2 + r_{mag}^2)}{\pi \mu_0 t_{mag}^2}\right]\frac{1}{2}\left(\begin{array}{c}\left[\frac{-1}{d_{2-1}^2} - \frac{1}{(d_{2-1}+2t_{mag})^2} + \frac{2}{(d_{2-1}+t_{mag})^2}\right] \\ + \left[\frac{-1}{d_{3-1}^2} - \frac{1}{(d_{3-1}+2t_{mag})^3} + \frac{2}{(d_{3-1}+t_{mag})^3}\right]\end{array}\right) + \frac{mv^2}{r}\right]x^2(3l-x)}{6EI} \cdot \frac{1}{6EI} \tag{13}$$

The velocity of air at the tip of the fan determined the value of Reynolds number, $Re$ which define the type of air flow due to the fan (Equation 14).

$$Re = \frac{vL_f}{\nu_a} = \frac{f_r \delta L_f}{\nu_a} \tag{14}$$

where is $L_f$ characteristic length of the fan and $\nu_a$ is the kinematic viscosity of the ambient air. The characteristic length of the piezoelectric fan is

$$L_f = \frac{4\delta W_m}{2(\delta + W_m)} \tag{15}$$

where, $A$ is the amplitude of the fan and $W_m$ is the width of the Mylar plate. For MPMF, the $Re$ is calculated as in [24]:

$$Re_{MPMF} = \frac{(f_r A L_f)_{MPMF}}{\nu_a} = \frac{\sum_{i=1}^{N} f_r A_i L_{f,i}}{N \nu_a} \tag{16}$$

The effect of air flow generated by multiple piezoelectric magnetic fans is considered small thus suit to cool a small or moderate power of electronic devices. The deflection of each fan might differ due to different magnetic force that transferred to the fan. Therefore, the Reynolds number for MPMF system is the average reading calculated using Equation (16). The range of Reynolds number determines the type of the air flow.

- Laminar $Re < 2300$
- Transient $2300 < Re < 4000$
- Turbulent $Re > 4000$

Based on [41], the air flow generated by single piezoelectric fan is laminar flow with the range of $680 \leq Re \leq 940$. Multiple fans in dual side array orientation had been done by [42] which recorded $0 \leq Re \leq 308$. A radial orientation of multiple fans has recorded $0 \leq Re \leq 301$ that has been done by [31]. Nusselt number, $Nu$ is the ratio of convection to conduction. The importance of $Nu$ in thermal analysis is we get to know the type of fluid motion whether it is laminar, transient or turbulent. $Nu = 1$ represents heat transfer by pure conduction. A value between 1 and 10 is characteristic of slug flow or laminar flow.

$$Nu = \frac{h L_h}{k_c} \tag{17}$$

where $h$ is heat convection coefficient, $L_h$ is length of heat source, $k_c$ is thermal conductivity. Another dimensionless number is Prandtl number, $Pr$; which indicates a dimensionless ratio between momentum diffusivity ($\nu$) and thermal diffusivity, $\alpha$.

$$Pr = \frac{c_p \mu}{k_c} = \frac{\nu}{\alpha} \tag{18}$$

For laminar flow, the Nusselt number can be expressed in terms of $Re$ and $Pr$

$$Nu_x = \frac{h_x x}{k} = 0.332 Re_x^{1/2} Pr^{1/3} \quad [0.6 \leqslant Pr \leqslant 50] \tag{19}$$

The total thermal resistance for MPMF is summation of thermal resistance due to conduction and convection heat transfer.

$$R_{tot} = R_{t,\,cond} + R_{t,\,conv} = \frac{L}{kA_{cond}} + \frac{1}{hA_{conv}} \tag{20}$$

The thermal resistance can also be described as a function of heat source power input

$$R_{t,\,conv} = \frac{T_{surface} - T_{ambient}}{Q - Q_c} \tag{21}$$

A good cooling system is a system that has small value of thermal resistance which indicate such cooling system approaching maximum efficiency. The thermal efficiency of MPMF can be measured by comparing the thermal resistance between natural convection and forced convection.

$$\eta = \left| \frac{R_c - R_n}{R_n} \right| \times 100\% \tag{22}$$

where, $R_c$ is thermal resistance of forced convection and $R_n$ is thermal resistance of natural convection. A dimensionless heat convection number introduced by [42] shows the ratio of heat convection coefficient under MPMF cooling system ($h_{MPMF}$) to the heat convection coefficient under natural convection ($h_0$.

$$M_{MPMF} = \frac{h_{MPMF}}{h_0} \tag{23}$$

The value of $M_{MPMF}$ indicated the performance of MPMF. MPMF is more than zero indicated the system has a better heat transfer compared to natural convection. The performance of piezoelectric fan also depends on the velocity generated at the fan tip.

### 3.1.2. Uncertainties

The dimensional error during cutting passive fans were estimated to be $\pm$ 0.1 mm. The accuracy of the temperature measurement by K-type thermocouples was $\pm$ 0.2 K; the uncertainties of power input was $\pm$ 1 W. The standard error of design (predicted mean) for such matrix table was between 0.378 and 0.8. The smaller the standard error, the more reliable the estimation. The standard error has provided a rough idea about the relative quality of predicted response values in various locations in the design region [33]. Radiation heat transfer sometimes can be neglected depends on the material used which is aluminium alloy. By calculation, the radiation heat transfer from the heat sink is very small in the range of 0.05 W to 1.93 W. Therefore, the heat loss through radiation in this study can be ignored.

## 4. Results and discussion

The significance of magnet can only be realized if more passive fans were added to the cooling system. The magnets were arranged facing the same poles (N—N or S—S) which generated repulsive magnetic forces between the magnets. The force was always in positive force [40] so that it is continuously enhancing the cumulative forces acting on the fan blades. The optimum value of distance between magnets can be obtained based on the deflection and velocity of air at the tip of the MPMF.

### 4.1. Design optimization

For multiple fans, the resonant frequency might be restricted by the distance between magnets that cause the fans cannot be operating at its resonance frequency. Therefore, the best frequency was selected based on the average deflection generated by each of the fans. Varying the distance in between gave different overall deflection that might complicate the optimization process. Less magnetic stiffness had caused the driving fan to deflect with higher amplitude but smaller frequency. Thus, the adjacent fans received lesser magnetic force and not able to have higher vibration to distract the air flow to improve the heat transfer.

The optimal value of $d$ was nominated based on maximum average deflection and maximum average velocity. Using RSM in Design Expert software (DE), a quadratic model was suggested with p-value < 0.0001. The significance of the model was evaluated by the correlation coefficient or coefficient of multiple determination, $R^2$ for the variables in charge; velocity of air and fan deflection.

The CCD has suggested 31 runs to complete the matrix table. The fit summary for both responses were combined together in Table 3. For both responses, the suggested model is quadratic and a new adjusted $R^2$ was recommended.

Fig. 5 shows the actual deflection and frequency at different distance between magnets and orientation. The purpose of selecting the optimum value of distance between magnets and location of magnet is to obtain the highest velocity of air generated at the tip of the fans. Each fan might have different velocity at the tip, depends on the deflection of the fan. The running frequency for passive fans is assumed to be the same as the

**Table 3**

Fit summary for responses deflection and average velocity.

| | Source | Model p- value | Adjusted R² | Predicted R² | |
|---|---|---|---|---|---|
| | **Design Model** | **< 0.0001** | **0.9808** | | **Recommended** |
| | Linear | 0.4913 | −0.0178 | −0.5581 | |
| Deflection | 2FI | 0.2393 | 0.0361 | −2.5457 | |
| | **Quadratic** | **< 0.0001** | **0.9729** | **0.8438** | **Suggested** |
| | Cubic | | 1.0000 | | Aliased |
| | **Design Model** | **< 0.0001** | **0.9762** | | **Recommended** |
| | Linear | 0.6151 | −0.0407 | −0.5476 | |
| Average velocity | 2FI | 0.7350 | −0.1114 | −3.1773 | |
| | **Quadratic** | **< 0.0001** | **0.9547** | **0.7089** | **Suggested** |
| | Cubic | | 1.0000 | | Aliased |
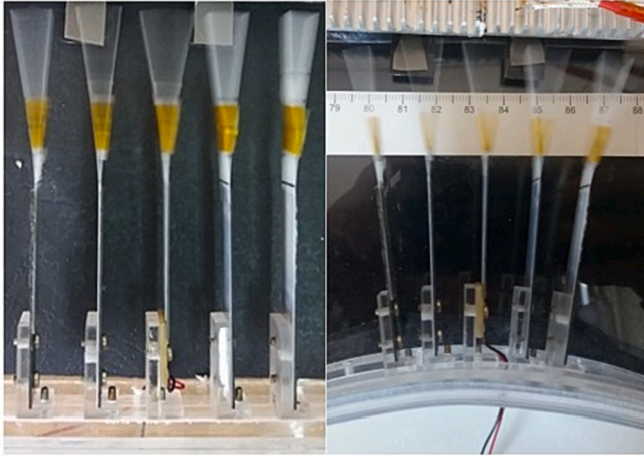


**Fig. 5.** Maximum deflection with optimum distance between magnets to length ratio.

driving fan.

The achievement of R² is very good since it is closed to 1 both for deflection and average velocity. Adjusted R² indicates the suggested equation was developed with significant variables or terms in the model equation. R² helped to avoid unnecessary variables to be included in the model equation. The predicted R² for deflection is in reasonable agreement with the adjusted R² since the difference is<0.2. On the other side, ANOVA analysis in Table 4 has suggested a significant model based on the F-value and p-value. From the analysis, P-value<0.0500 indicates the model terms are significant to be listed in the equation.

The final coded equation of deflection and velocity for each orien-

tation; array and radial are recorded for validation later. $A$ is for frequency offset and $B$ is for location of magnet.

$$\Delta\delta_{(a)} = -16.89039 - 0.505100A + 1.20945B - 0.055172AB + 0.006942A^2 - 0.118335B^2 \tag{24}$$

$$\Delta\delta_{(r)} = 11.1043 - 0.239242A + 1.04945B - 0.055172AB + 0.006942A^2 - 0.118335B^2 \tag{25}$$

$$\Delta vel_a = -3.64062 + 0.423301A + 0.105447B - 0.005259AB - 0.009044A^2 - 0.013507 B^2 \tag{26}$$

$$\Delta vel_r = -4.06038 + 0.44538A + 0.106947B - 0.005259AB - 0.009044A^2 - 0.013507B^2 \tag{27}$$

The interaction between frequency offset and deflection with distance between magnet and the velocity profile as the response for frequency offset and $d$ can be viewed in Fig. 6. At fixed $d$ value, the maximum deflection always occurred at frequency offset equals 0 %. The deflection decreases as $d$ is larger.

The curve is converged compared to deflection profile but still having similar interpretation. At fixed $d$ value, the maximum velocity is at maximum at 0 % of frequency offset. The optimization tool in RSM has helped to suggest the optimum $d$ value with the influence of responses deflection and average velocity. According to Fig. 7, the optimal $d$ value is 22.70 % which was 15.66 mm.

The determination of upper and lower limit of $d$ value is based on initial results. The result is more accurate for smaller range between the upper and lower limit. The initial results were selected based on the desired average fan deflection of MPMF. The $d$ value is selected in such a way that each of the fans are deflecting at more or less similar deflection so that the air velocity at the tip of the fan also in average reading. The



(a)



(b)
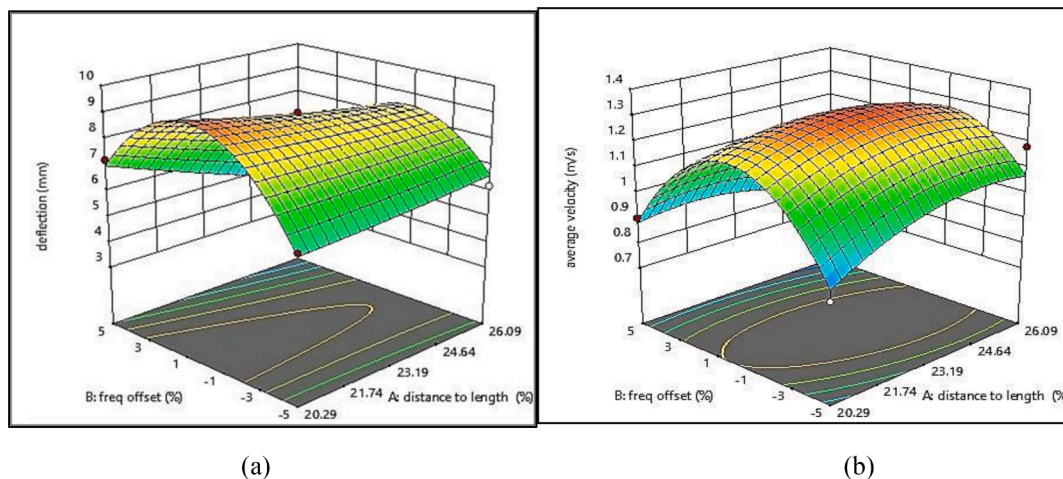
**Fig. 6.** (a) Average deflection and (b) average velocity with variation of distance between magnets.
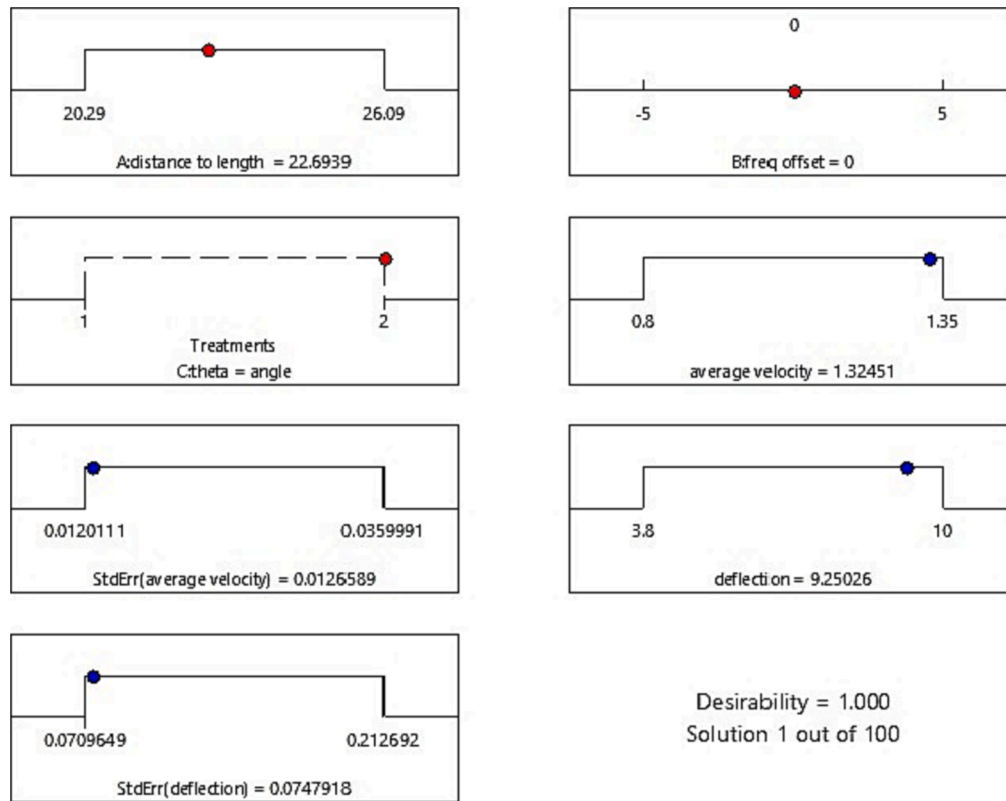
Fig. 7. Optimization of responses average velocity and deflection.

**Table 4**
Upper limit and lower limit for factor distance between magnets to length ratio.

| Test | Lower limit, mm | Upper limit, mm |
|------|-----------------|-----------------|
| I    | 12              | 18              |
| II   | 12              | 16              |
| III  | 12              | 15              |
| IV   | 12              | 14              |

**Table 5**
Frequency for APMF and RPMF.

| $d$, mm | Frequency, Hz | |
| | APMF | RPMF |
|---------|------|------|
| 12 | 40.22 | 42.66 |
| 14 | 37    | 40.25 |
| 16 | 35.1  | 36.5  |
| 18 | 34.5  | 34.6  |

similar steps in RSM were repeated at different upper and lower limit as shown in Table 4.

In conclusion, as the range of the distance between magnet becomes smaller, higher accuracy was achieved. Therefore, the optimized $d$ value using RSM is 21.01 % equivalent to 14.5 mm. The deflection of fans on different orientation at different heat power input is shown in Table 5.

As the gap between fans is closer, the frequency became higher. At the same distance between magnets, the RPMF had consistently achieved higher frequency compared to APMF due to RPMF obtained extra force from its orientation known as centrifugal force. Therefore, instead of enlarging the cooling coverage area, RPMF also has increased the frequency of the RPMF at same distance between magnets in APMF.

Therefore, the optimization of distance between magnets to fan length ratio, $d$ is defined as the potential design parameter that directly influence the performance of MPMF. The selection of the optimum

distance between magnets was based on the widest average deflection can be made by the multiple fans at highest running frequency to gain the largest average velocity of air that could be generated by the fans. The optimization was done using Response Surface Method (RSM). The test was based on deflection and average air velocity. All the fan blades need to have more or less same deflection to generate a consistent air velocity at the tip of the fan so that the hot air continuously flowing out from the operating device [43]. The frequency of RPMF is consistently larger than APMF provided the $d$ value is same. High frequency generates larger air velocity thus, RPMF is perceived faster than linear motion [44].

### 4.2. Thermal performance of MPMF

The innovation of MPMF has enlarged the cooling coverage area compared to single fan (762 mm$^2$), where APMF and RPMF covered 2475 mm$^2$ and 3405 mm$^2$ respectively. In thermal analysis, the MPMF is always running at its best condition by applying the optimal values of selected parameters. The optimal location of magnet is x = 44 mm and the distance between magnets to length ratio is 14.5 mm. Such orientation generated air flow with different Reynolds number depending on the resonant frequency, the average wavelength of the MPMF and the viscosity of air. The viscosity of air increase with the increment of temperature and the temperature increment is proportional to the input power increment. Therefore, as the heat power input increase, the Reynolds number decreased, provided there is no adjustment on the performance of the MPMF.

As for the Prandtl number, since it is the ratio of momentum to the thermal diffusivities, the value can be obtained from the thermophysical properties table. The value reduced if there is increment in temperature. Fig. 8 summarized the changes of Nusselt number and Reynolds number as the input power increased. The MPMF is operating at its maximum performance while the temperature of the heat source increased. Therefore, the Nu and Re decreased as the input power
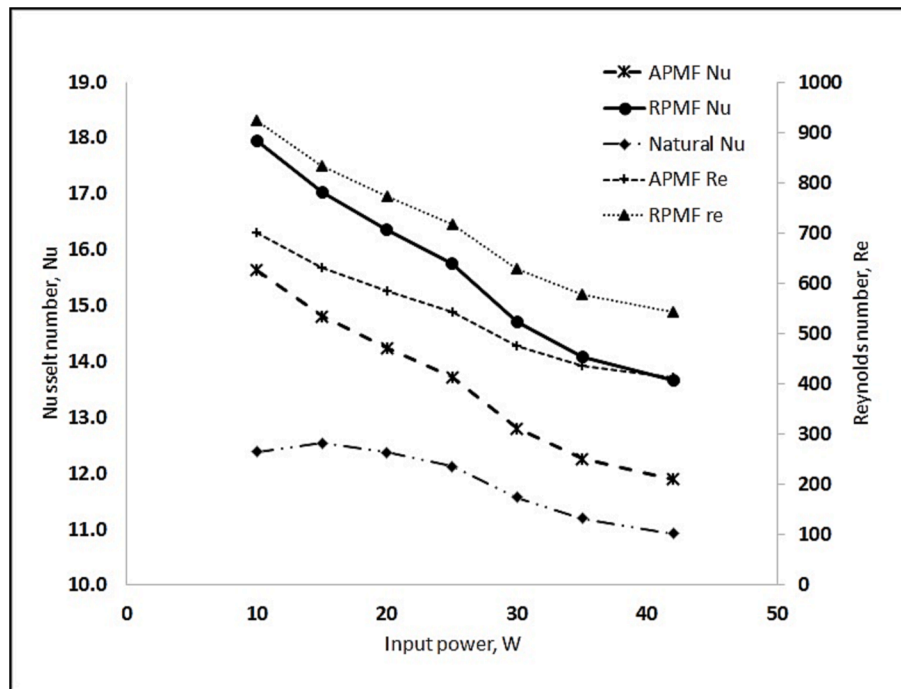
**Fig. 8.** Comparison of Nusselt number and Reynolds number to the heat input power.
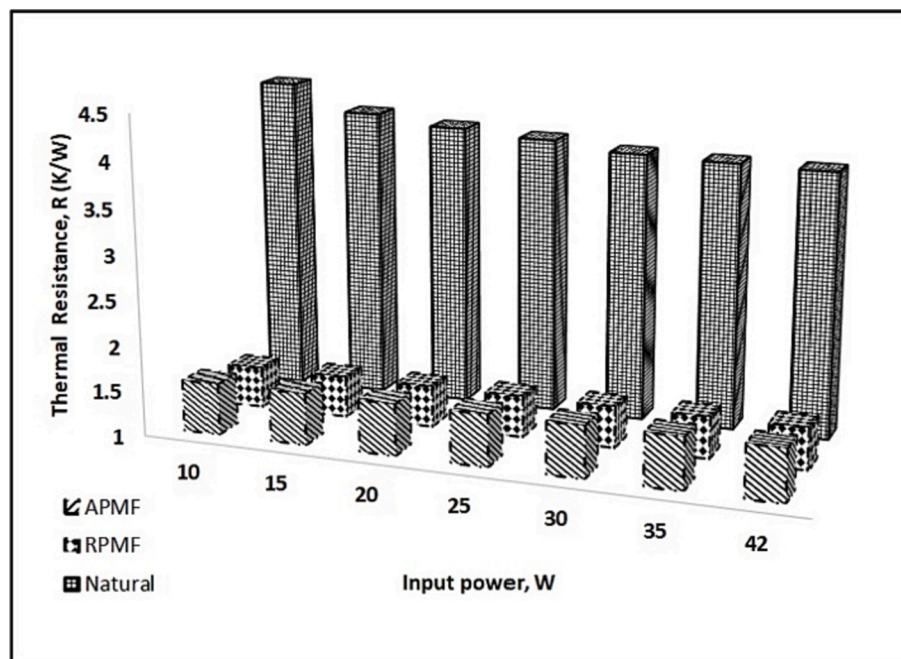


**Fig. 9.** Comparison of thermal resistance between natural convection, APMF.

increased due to the MPMF cooling system is fixed and noted that the thermal properties of RPMF is consistently higher than APMF. As the Nu and Re correspond to a more active convection heat transfer, higher Nu and Re is desired for a better cooling system. At 25 W, the APMF Nu and RPMF Nu are improved by 13 % and 30 % respectively compared to natural convection. The RPMF has improved Nu by 130 % compared APMF. The RPMF Re has improved the APMF Re by 32 %.

The heat transfer is associated with thermal resistance and in this case, only thermal resistance due to convection is considered. Higher thermal resistance means the heat is difficult to be removed. At constant power input, the thermal resistance could be reduced by increasing the

surface area of the heat source and the heat convection coefficient which proportional with the Nusselt number. The improvement of Nusselt number of RPMF is very significant as it shows almost double increment compared to APMF. In conclusion, as the Nusselt number improved for the RPMF, the proposed orientation also has reduced the thermal resistance for the heat to be transferred out. Fig. 9 displayed the thermal resistance for each orientation and large reduction compared to the natural convection. The RPMF has reduced the thermal resistance by 7.6 % compared to APMF. Besides having advantages to cover a larger cooling area, RPMF also has improved the cooling performance while maintaining the power consumption of 30 mW.
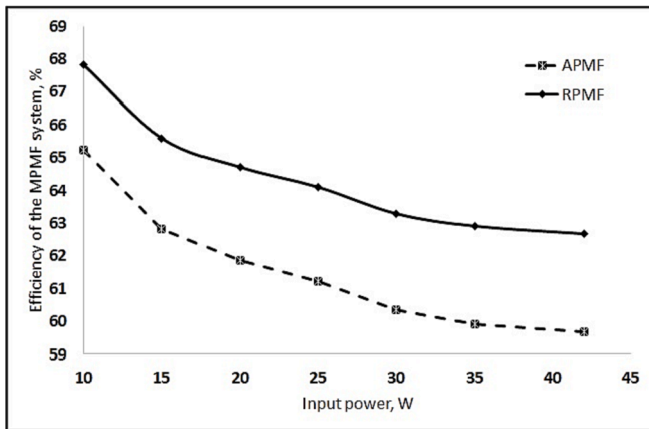
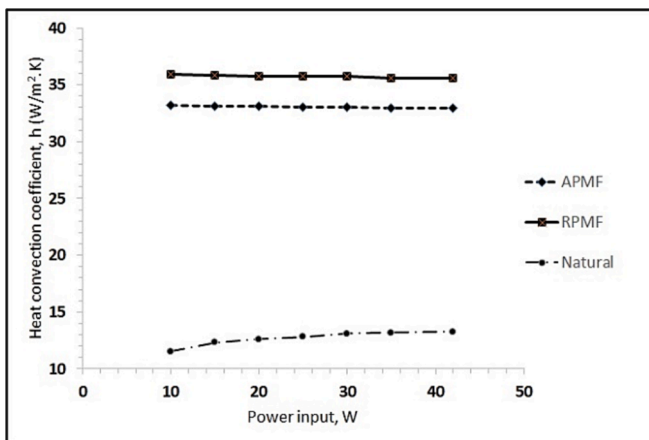**Fig. 10.** Comparison of thermal efficiency between APMF and RPMF.



**Fig. 11.** Comparison of heat convection coefficient for APMF and RPMF.

The reduction in thermal resistance can also denoted as the overall efficiency of the MPMF system as indicated in Fig. 10. The RPMF is 5 % more efficient than APMF in cooling the heat source. However, in overall, the efficiency reduced as the power input increased which means that the MPMF is limited to small scale of electronic device.

Fig. 11 shows the RPMF is constantly getting higher h value compared to APMF. The enhancement of heat convection coefficient is due to the average velocity developed at the fan tip. At same distance between magnets, the RPMF able to generate higher resonant frequency and slightly wider deflection compared to APMF. The frequency is higher due to additional centrifugal force due to radial orientation. The centrifugal force also contributes to increase the magnetic stiffness between the fans. By changing the orientation, it helps to increase the heat convection coefficient by 3 $W/m^2K$ which is equivalent to 9.1 %. The advantage of MPMF is it able to distribute the moving air in a wider area compared to single fan. The Reynolds number for single fan is larger than MPMF due to higher resonant frequency thus led to greater velocity. MPMF produced lower frequency because of additional load consisted of passive fan and magnets but the performance of MPMF can be enhanced by changing the driving piezoelectric fan to a higher frequency so that the heat transfer rate can be improved.

The improvement of convective heat transfer can be represented by the dimensionless heat convection number, $M_{MPMF}$ as shown in Fig. 12. The $M_{MPMF}$ is decreased when the heat size increased. This indicates that as the input power become larger, it reduces the performance of MPMF cooling system until there is no more cooling effect due to MPMF and the natural convection will take over.

## 5. Conclusion

An equation of total force applied on each fan equipped with magnet has been derived. The equation of magnetic force between the magnet is applicable at any situation, array and radial orientation. During experimental data collection, the frequency of RPMF is always greater than APMF; provided the distance between magnets for both orientations is the same. This is due to the difference on the centrifugal and centripetal force existed for RPMF that cause the magnetic stiffness for RPMF is a bit
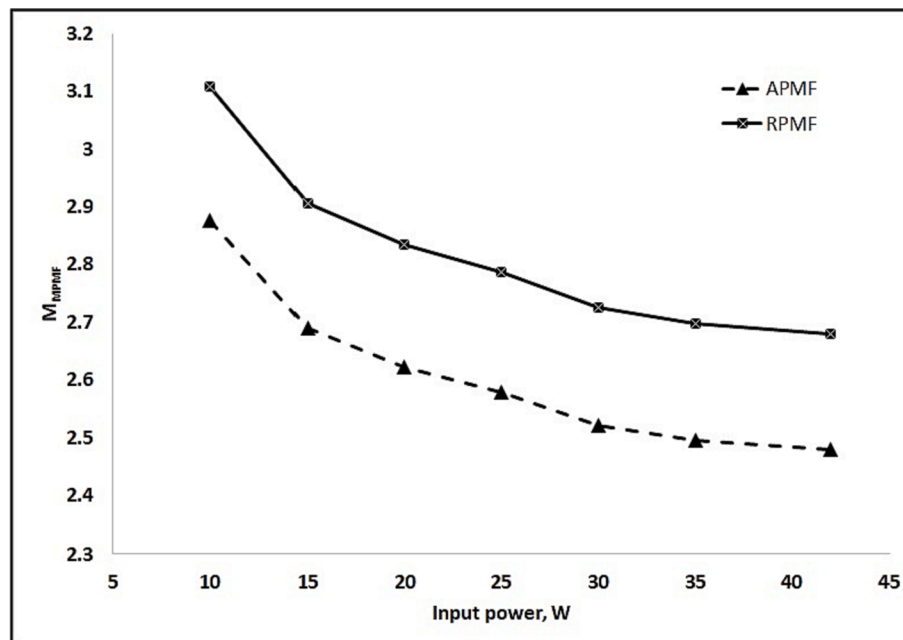


**Fig. 12.** Comparison of dimensionless coefficient between AMPF and RPMF.

stronger than APMF. As for MPMF in general, the optimal magnet location was applied to all the fans. The optimization of distance between magnets is achieved when the fans deflect almost at the same magnitude so that the average velocity of air could be transferred efficiently to the area covered by each fan. The optimal result produced by DE is $d$ = 14.5 mm- 16.5 mm. At $d$ = 14.5 mm, the frequency for RPMF and APMF are 42.66 Hz and 40.25 Hz respectively. Average fan deflection for both orientations is 10.2 mm and 9.8 mm respectively. The determination of the best orientation of MPMF was conducted using DE and the result agrees with the outcome from the previous test. The optimized MPMF could be implemented on a projectors or drones that have limited space for cooling system and require minimum noise level during the operation.

## CRediT authorship contribution statement

**Fadhilah Abdul Razak:** Conceptualization, Data curation, Formal analysis, Investigation, Methodology, Visualization, Writing – original draft, Writing – review & editing. **Robiah Ahmad:** Conceptualization, Funding acquisition, Methodology, Project administration, Resources, Supervision, Validation, Writing – review & editing. **Shamsul Sarip:** Conceptualization, Funding acquisition, Methodology, Project administration, Resources, Supervision, Validation, Writing – review & editing. **Firdaus Muhammad-Sukki:** Funding acquisition, Supervision, Visualization, Writing – review & editing.

## Declaration of Competing Interest

The authors declare that they have no known competing financial interests or personal relationships that could have appeared to influence the work reported in this paper.

## Data availability

Data will be made available on request.

## Acknowledgement

## References

[1] D. Anderson, J.C. Tannehill, R.H. Pletcher, Computational fluid mechanics and heat transfer., 3rd Editio, 2016. 10.2307/2008017.

[2] G. Hetsroni, A. Mosyak, Z. Segal, G. Ziskind, A uniform temperature heat sink for cooling of electronic devices, Int. J. Heat Mass Transf. 45 (2002) 3275–3286, https://doi.org/10.1016/S0017-9310(02)00048-0.

[3] S.A. Jajja, W. Ali, H.M. Ali, Multiwalled carbon nanotube nanofluid for thermal management of high heat generating computer processor, Heat Transf. - Asian Res. 43 (2014) 653–666, https://doi.org/10.1002/htj.21107.

[4] M.J. Moran, H.N. Shapiro, B.R. Munson, D.P. DeWitt, Introduction to Thermal Systems Engineering: Thermodynamics, Fluid Mechnics and Heat Transfer (2003), https://doi.org/10.1080/17415970600573619.

[5] M.A. Ebadian, C.X. Lin, A Review of High-Heat-Flux Heat Removal Technologies, J. Heat Transfer. 133 (2011) 1–11, https://doi.org/10.1115/1.4004340.

[6] Y.H. Liu, S.Y. Tsai, C.C. Wang, Effect of driven frequency on flow and heat transfer of an impinging synthetic air jet, Appl. Therm. Eng. 75 (2015) 289–297, https://doi.org/10.1016/j.applthermaleng.2014.09.086.

[7] M. Arik, Y. Utturkar, Interaction of a synthetic jet with an actively cooled heat sink, in: 2008 11th Intersoc. Conf. Therm. Thermomechanical Phenom. Electron. Syst., IEEE, 2008: pp. 374–379. 10.1109/ITHERM.2008.4544294.

[8] C. Wang, Thermal Management for Portable Electronics Using a Piezoelectric Micro-Blower, 19 (2019) 563–567.

[9] A.R. Fadhilah, A. Robiah, S. Shamsul, Thermal analysis of radial piezoelectric-magnetic fan (RPMF) for electronics cooling, Int. J. Integr. Eng. 10 (2018) 140–147. 10.30880/ijie.2018.10.07.013.

[10] T. Acikalin, S.M. Wait, S.V. Garimella, A. Raman, T. AÇIKALIN, S.M. Wait, S. V. Garimella, A. Raman, Experimental Investigation of the Thermal Performance of Piezoelectric Fans, Heat Transf. Eng. 25 (2004) 4–14, https://doi.org/10.1080/01457630490248223.

[11] J.H. Yoo, J. Il Hong, W. Cao, Piezoelectric ceramic bimorph coupled to thin metal plate as cooling fan for electronic devices, Sensors Actuators A Phys. 79 (2000) 8–12, https://doi.org/10.1016/S0924-4247(99)00249-6.

[12] K. Tseng, M. Mochizuki, K. Mashiko, Piezo fan for thermal management of electronics, Fujikura Tech. Rev. (2010) 39–43.

[13] C.-N. Lin, J.-Y. Jang, J.-S. Leu, A Study of an Effective Heat-Dissipating Piezoelectric Fan for High Heat Density Devices, Energies. 9 (2016) 610, https://doi.org/10.3390/en9080610.

[14] A.R. Fadhilah, A. Robiah, S. Shamsul, High potential of magnet on the performance of dual piezoelectric fans in electronics cooling system, Indones. J. Electr. Eng. Comput. Sci. 10 (2018) 469–479. 10.11591/ijeecs.v10.i2.pp469-479.

[15] S. Liu, R. Huang, W. Sheu, C. Wang, Heat transfer by a piezoelectric fan on a flat surface subject to the influence of horizontal/vertical arrangement, Int. J. Heat Mass Transf. 52 (2009) 2565–2570, https://doi.org/10.1016/j.ijheatmasstransfer.2009.01.013.

[16] J.-C. Shyu, J. Syu, Plate-fin array cooling using a finger-like piezoelectric fan, Appl. Therm. Eng. 62 (2014) 573–580, https://doi.org/10.1016/j.applthermaleng.2013.10.021.

[17] Y. Yu, T.W. Simon, M. Zhang, T. Yeom, M.T. North, T. Cui, Enhancing heat transfer in air-cooled heat sinks using piezoelectrically-driven agitators and synthetic jets, Int. J. Heat Mass Transf. 68 (2014) 184–193, https://doi.org/10.1016/j.ijheatmasstransfer.2013.09.001.

[18] T.J. Liu, Y. Chen, H. Ho, J. Liu, C. Lee, Notes on vibration design for piezoelectric cooling, Int. J. Mech. Aerospace, Ind. Mechatron. Manuf. Eng. 7 (2013) 294–298.

[19] L. Tan, J. Zhang, H. Xu, Jet impingement on a rib-roughened wall inside semi-confined channel, Int. J. Therm. Sci. 86 (2014) 210–218, https://doi.org/10.1016/j.ijthermalsci.2014.06.037.

[20] S.F. Sufian, M.Z. Abdullah, M.K. Abdullah, J.J. Mohamed, Effect of Side and Tip Gaps of a Piezoelectric Fan on Microelectronic Cooling, IEEE Trans. Components, Packag. Manuf. Technol. 3 (2013) 1545–1553, https://doi.org/10.1109/TCPMT.2013.2251759.

[21] M.K. Abdullah, N.C. Ismail, M.Z. Abdullah, M.A. Mujeebu, K.A. Ahmad, Z.M. Ripin, Effects of tip gap and amplitude of piezoelectric fans on the performance of heat sinks in microelectronic cooling, Heat Mass Transf. 48 (2012) 893–901, https://doi.org/10.1007/s00231-011-0944-z.

[22] I. Sauciuc, S. Ahuja, G. Ashish, Piezo fans for cooling an electronic device, US 2009/0279255 A1, 2009.

[23] T. Yeom, T.W. Simon, L. Huang, M.T. North, T. Cui, Piezoelectric-translational-agitation-for-enhancing-forced-convection-channel-flow-heat-transfer, Int. J. Heat Mass Transf. 55 (25-26) (2012) 7398–7409.

[24] H.K. Ma, S.K. Liao, B.T. Lin, Application of multiple fans with a piezoelectric actuator system inside a pico projector, Int. Commun. Heat Mass Transf. 78 (2016) 80–87, https://doi.org/10.1016/j.icheatmasstransfer.2016.08.018.

[25] H.K. Ma, S.K. Liao, Y.T. Li, Y.F. Li, C.L. Liu, The application of micro multiple piezoelectric-magnetic fans (m-MPMF) on LEDs thermal management, Annu. IEEE Semicond. Therm. Meas. Manag. Symp. (2014) 159–163, https://doi.org/10.1109/SEMI-THERM.2014.6892233.

[26] H.K. Ma, H.C. Su, C.L. Liu, W.H. Ho, Investigation of a piezoelectric fan embedded in a heat sink, Int. Commun. Heat Mass Transf. 39 (2012) 603–609, https://doi.org/10.1016/j.icheatmasstransfer.2012.03.003.

[27] H.K. Ma, Y.T. Li, S.Y. Ke, C.P. Lin, The role of housing design in a multiple fans system with a piezoelectric actuator, Appl. Therm. Eng. 91 (2015) 986–993, https://doi.org/10.1016/j.applthermaleng.2015.08.049.

[28] A.R. Fadhilah, A. Robiah, S. Shamsul, An investigation of magnet parameters on the performance of dual piezoelectric fans (DPF) in electronics cooling system, in: 4th Int. Conf. Smart Instrumentation, Meas. Appl., 2017: pp. 1–6. 10.1109/ICSIMA.2017.8311998.

[29] H.K. Ma, L.K. Tan, Y.T. Li, Investigation of a multiple piezoelectric – magnetic fan system embedded in a heat sink, Int. Commun. Heat Mass Transf. 59 (2014) 166–173, https://doi.org/10.1016/j.icheatmasstransfer.2014.10.002.

[30] A.R. Fadhilah, A. Robiah, S. Shamsul, Investigation of Radial Piezoelectric-Magnetic Fan for Electronic Cooling System, in: 2018 2nd Int. Conf. Smart Sensors Appl. ICSSA 2018, 2018: pp. 116–119. 10.1109/ICSSA.2018.8535929.

[31] H.K. Ma, S.K. Liao, C.H. Hsieh, Development of a radial-flow multiple magnetically coupled fan system with one piezoelectric actuator, Int. Commun. Heat Mass Transf. 87 (2017) 212–219, https://doi.org/10.1016/j.icheatmasstransfer.2017.07.018.

[32] Fadhilah, A. Razak, Robiah, Ahmad, Shamsul, Sarip, Optimization of Location of Magnet on Multiple Piezoelectric-Magnetic Fan (MPMF) using Design Expert, 2019 IEEE 6th Int. Conf. Smart Instrumentation, Meas. Appl. ICSIMA 2019. (2019). 10.1109/ICSIMA47653.2019.9057341.

[33] R.H. Myers, D.C. Montgomery, C.M. Anderson-Cook, Response Surface Methodology, 3rd ed.,, John Wiley and Sons Inc, 2009.

[34] A.R. Fadhilah, A. Robiah, S. Shamsul, Investigation of Radial Piezoelectric-Magnetic Fan (RPMF) Performance for Electronic Cooling System, in: ICSSA, 2018.

[35] Y. Cao, X.B. Chen, A Survey of Modeling and Control Issues for Piezo-electric Actuators, J. Dyn. Syst. Meas. Control. 137 (2015), 014001, https://doi.org/10.1115/1.4028055.

[36] Z.M. Fairuz, S.F. Su, M.Z. Abdullah, M. Zubair, M.S.A. Aziz, Effect of piezoelectric fan mode shape on the heat transfer characteristics, Int. Commun. Heat Mass Transf. 52 (2014) 140–151, https://doi.org/10.1016/j.icheatmasstransfer.2013.11.013.

[37] V. Piefort, Finite Element Modelling of Piezoelectric Active Structures, Universite Libre de Bruxelles (2001).

[38] S.F. Sufian, Z.M. Fairuz, M. Zubair, M.Z. Abdullah, J.J. Mohamed, Thermal analysis of dual piezoelectric fans for cooling multi-LED packages, Microelectron. Reliab. 54 (2014) 1534–1543, https://doi.org/10.1016/j.microrel.2014.03.016.

[39] X.-J. Li, J. Zhang, X. Tan, Effects of blade shape on convective heat transfer induced by a piezoelectrically actuated vibrating fan, Int. J. Therm. Sci. 132 (2018) 597–609, https://doi.org/10.1016/j.ijthermalsci.2018.06.036.

[40] H.K. Ma, H.C. Su, W.F. Luo, Investigation of a piezoelectric fan cooling system with multiple magnetic fans, Sensors Actuators A Phys. 189 (2013) 356–363, https://doi.org/10.1016/j.sna.2012.09.009.

[41] M. Kimber, S.V. Garimella, A. Raman, Local Heat Transfer Coefficients Induced by Piezoelectrically Actuated Vibrating Cantilevers, J. Heat Transfer. 129 (2007) 1168, https://doi.org/10.1115/1.2740655.

[42] H.K. Ma, Y.T. Li, Thermal performance of a dual-sided multiple fans system with a piezoelectric actuator on LEDs, Int. Commun. Heat Mass Transf. 66 (2015) 40–46, https://doi.org/10.1016/j.icheatmasstransfer.2015.05.008.

[43] F.P. Incropera, D.P. Dewitt, T.L. Lavine, A.S. Bergman, Fundamental of heat and mass transfer, 6th editio, John Wiley and Sons, 2007.

[44] R.A. Champion, L. Evans, P.A. Warren, The effect of eccentricity on the linear-radial speed bias : Testing the motion-in-depth model, Vision Res. 189 (2021) 93–103, https://doi.org/10.1016/j.visres.2021.09.001.